

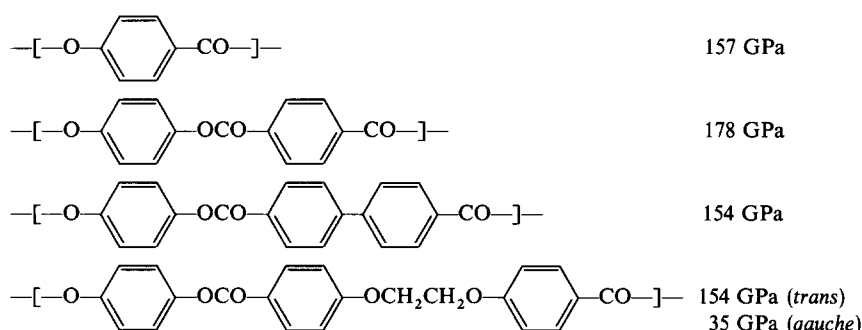
Lattice-dynamical prediction of the limiting Young's modulus of liquid crystalline arylate polymers: comparison with typical rigid-rod polymers

Kohji Tashiro* and Masamichi Kobayashi

Department of Macromolecular Science, Faculty of Science, Osaka University, Toyonaka, Osaka 560, Japan

(Received 28 December 1989; revised 29 January 1990; accepted 5 February 1990)

Based on the lattice dynamical equations, the theoretical Young's modulus E_l has been calculated for a series of arylate polyesters:



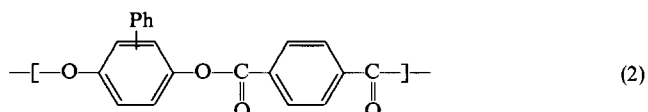
The calculated results have been interpreted in connection with the mechanical deformation mechanism of the chains based on the concept of strain energy distribution to the internal displacement coordinates such as bond lengths, bond angles and internal rotations. Although the arylate polyesters are constructed by a series connection of rigid benzene and ester groups, the calculated moduli are only one third of the modulus predicted for a completely linear polymer chain such as poly-*p*-phenylene. This originates from the characteristic structure of the arylate polymers. The straight aromatic segments are tilted from the chain axis due to the existence of the ester group and, therefore, the strain energy concentrates mainly on the weak bond angle deformation of the ester groups and distributes only slightly to the benzene ring deformation. That is, the rigidity of the aromatic rings has been found not to be used as effectively as expected from the chemical structures. Comparison of the Young's modulus and molecular deformation mechanism has been made between the present liquid crystalline polymers and polymers with various types of chain conformation, including poly-*p*-phenylene terephthalamide (calc. modulus 182 GPa, X-ray obs. 200 GPa) and poly-*p*-phenylene benzobisthiazole (calc. 392 GPa, X-ray obs. 395 GPa).

(Keywords: arylate polyesters; theoretical Young's modulus; lattice dynamics; molecular deformation mechanism; potential energy distribution)

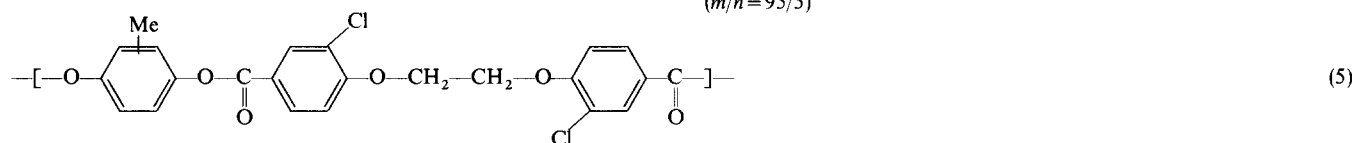
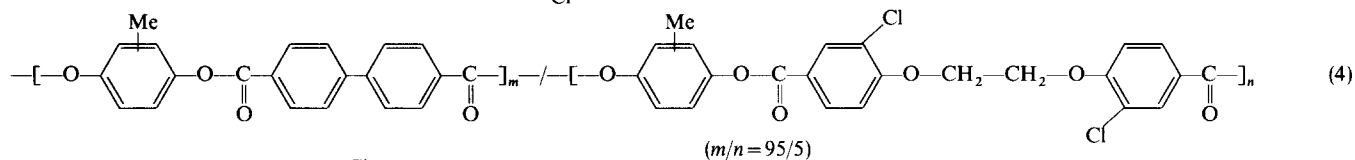
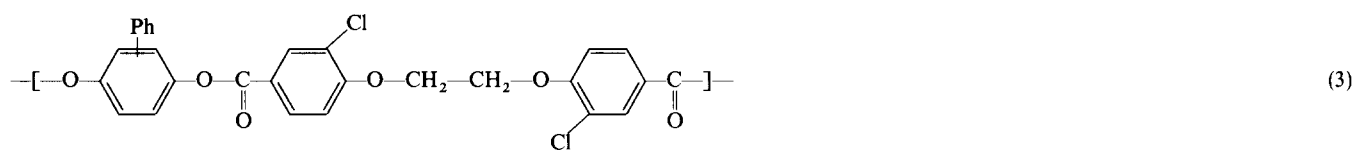
INTRODUCTION

Liquid crystalline arylate polymers have attracted attention recently because of their high processability from the melt and the high strength and high elastic modulus of the resultant fibres¹. Many types of chemical structure have been designed and synthesized for the polyarylates. But these trials have not been designed to search systematically for mechanically excellent polymers. One of the most important and constructive procedures in designing a mechanically superior polymer may be an evaluation of the exact limiting Young's modulus of these polyarylates and clarification of the relationship between elastic property and molecular conformation. In the

present paper, the theoretical modulus along the chain axis will be calculated, based on the lattice dynamical method^{2,3}, for five typical polyarylates with the following chemical structures:



* To whom correspondence should be addressed



The results will be discussed in relation to the molecular deformation mechanism of polymer chains under tension and some factors governing the modulus of these polyarylate systems will be extracted.

X-RAY FIBRE DIAGRAMS AND MOLECULAR STRUCTURE

Sample 1 was supplied by Toyobo Co. Ltd, Japan (in the form of single-crystal-like whiskers^{4,5}) and by Sumitomo Chemical Industry Co. Ltd, Japan (Ekonol[®]). Samples 2–5 were supplied by the Research Association of Polymer Basic Technology in Japan. Samples 2–5 were melted and spun into fibres. Figure 1 shows the electron diffraction pattern for sample 1 (whisker). Figure 2 shows X-ray fibre diagrams for as-spun fibres of samples 2–5. Sample 3 gives the amorphous halo X-ray pattern. The X-ray diagrams of samples 2, 4 and 5 exhibit a high degree of chain orientation, although the patterns are mostly broad, suggesting not a very high degree of crystallinity. The fibre periods estimated from Figures 1 and 2 are shown in Table 1.

It is not easy to speculate on the molecular conformation of these polymers only from fibre periods thus estimated. In the present case of wholly aromatic polyesters, however, the degree of freedom for the internal rotations around the skeletal backbones is not high, as understood from the chemical structures. Therefore, the possible molecular models may be limited. In the process of constructing suitable models, the chemical structures were simplified so that essential features were not lost; side groups such as phenyl, methyl, or chlorine atoms

were neglected. For copolymer sample 4, only the monomer sequences including the biphenyl groups are extracted by taking into account the molar ratio of the comonomers. In this way, the above-mentioned five samples may be represented by the following simplified

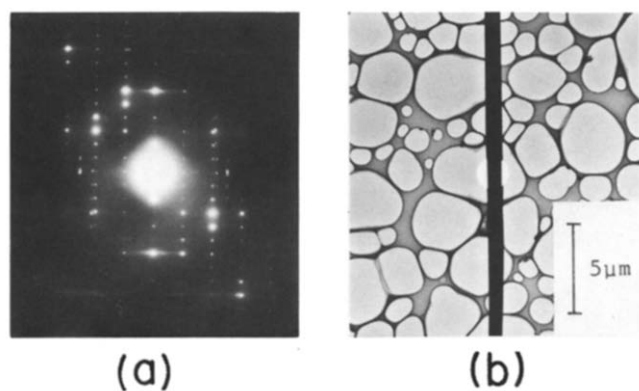


Figure 1 (a) Electron diffraction pattern of poly-*p*-oxybenzoyl whisker and (b) TEM image

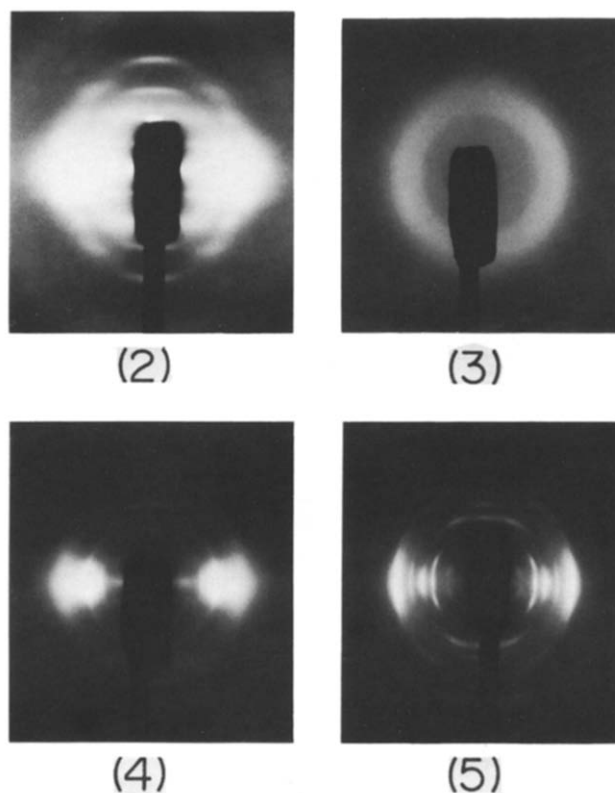


Figure 2 X-ray fibre diagrams for liquid crystalline polymer samples 2–5

Table 1 Fibre periods estimated from Figures 1 and 2

Sample	I_{obs} (\AA^a)
1	12.54 ^{4,5}
2	12.7
3	—
4	17.1
5	20.5

^a1 $\text{\AA} = 10^{-1}$ nm

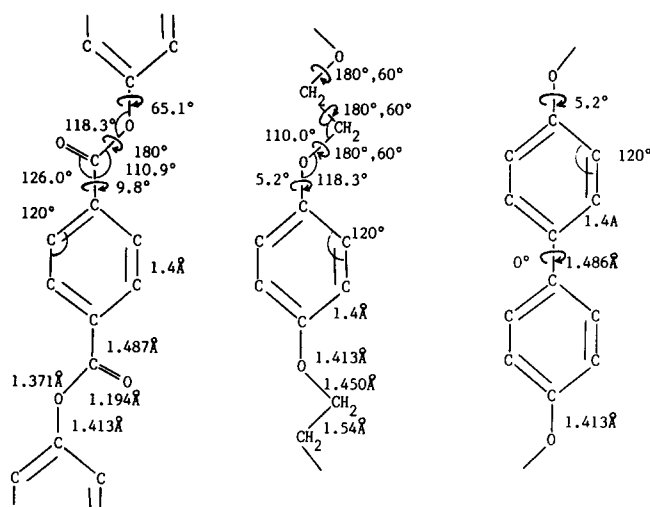
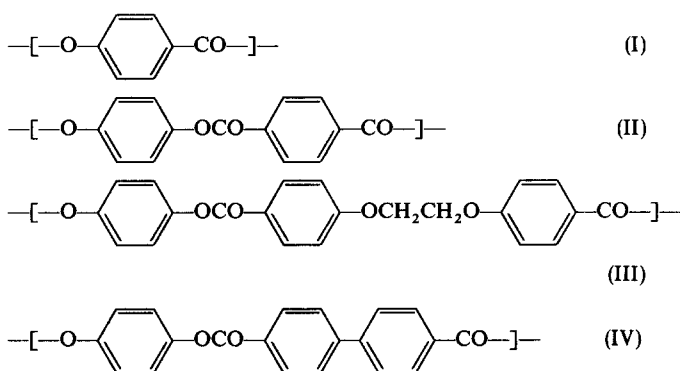


Figure 3 Molecular parameters for arylate polymer systems

model structures:



In the process of searching for a suitable molecular structural model, the bond lengths, bond angles and internal rotational angles are transferred from X-ray data analysed for both low molecular weight compounds⁶⁻⁹ and polymer systems¹⁰ with similar chemical structures (for example, poly(ethylene terephthalate) and poly(ethylene oxybenzoate)). Figure 3 shows the parameters used in the present calculation. The observed and calculated fibre periods are compared below for each polymer model.

Sample 1, model I

The fibre period of poly-*p*-oxybenzoyl (POB) is 12.54 Å as measured by electron diffraction of the micrometre-sized whisker (see Figure 1), suggesting that the two monomeric units are included in the repeating period^{4,5}. The most extreme model may be a planar conformation with *cis* or *trans* structure with respect to the relative direction of the C=O carbonyl groups (Figure 4). But the non-bonded interatomic interaction requires an energetically stable structure in which the ester group is twisted from the phenylene plane. The calculated fibre period of the *cis* planar model is 12.52 Å, and it becomes shorter when the phenylene group is twisted around the ester-benzene linkage: the agreement between calculated and observed period is worse. On the other hand, skeletal twisting in the *trans* planar model ($I_{calc} = 12.79$ Å) results in the contracted torsional model with a fibre period of

12.59 Å, in good agreement with the observed value, ≈ 12.54 Å. This torsional model is shown in Figure 4c.

Sample 2, model II

This polymer chain is considered to possess a point of symmetry at the centre of the benzene ring. The most plausible structural model obtained is shown in Figure 5. The calculated fibre period $I_{calc} = 12.76$ Å is in good agreement with the X-ray observed value of ≈ 12.7 Å.

Sample 4, model IV

Copolymer sample 4 is approximated as model IV. The torsional angle about the linkage connecting the two benzene rings of the biphenyl group may be dependent on environmental conditions, but in the present model it is assumed to be coplanar, as frequently observed. The fibre period calculated for model IV is 16.94 Å, which is consistent with the observed value of ≈ 17.1 Å within experimental error. When the biphenyl group is replaced by a virtual bond, the structure is essentially the same

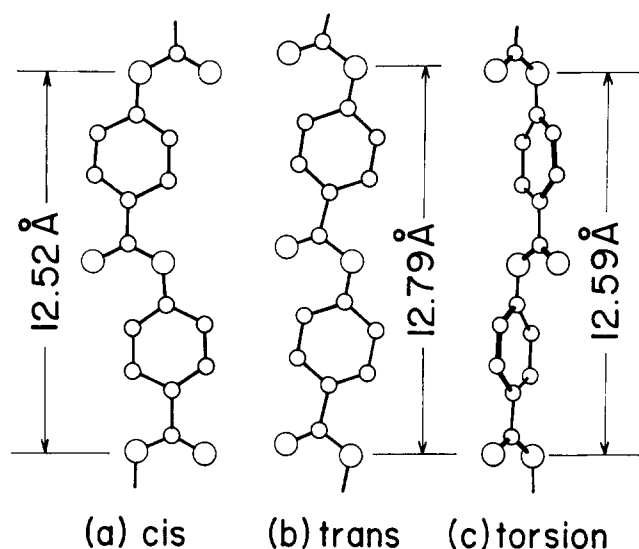


Figure 4 Molecular structure models for poly-*p*-oxybenzoyl: (a) *cis*; (b) *trans*; (c) torsion

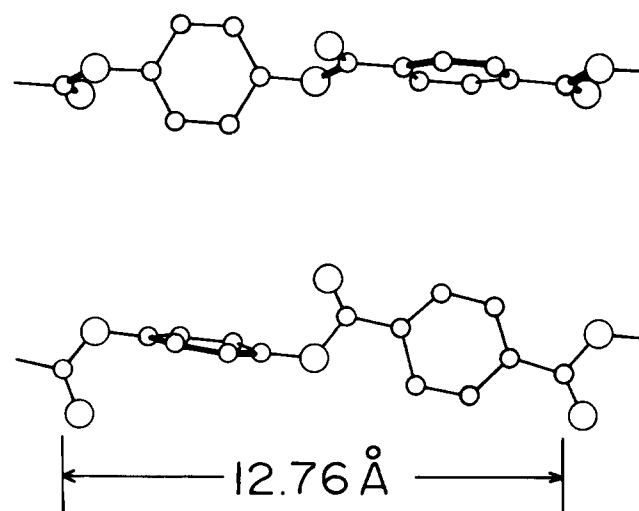


Figure 5 Molecular structure of model II

as that of model II, i.e. an all-*trans* zig-zag structure with different bond lengths (Figure 6).

Sample 5, model III

Model III contains a glycol group $-\text{OCH}_2\text{CH}_2\text{O}-$ in the skeletal chain. As expected, this glycol group is flexible and takes a variety of conformations: in poly(ethylene terephthalate) (PET) an all *trans* conformation, and in poly(ethylene oxybenzoate) (PEOB) two types of conformation, all *trans* (β form) and *gauche* (α form)¹⁰. Figure 7 shows the possible structural models, in which the glycol group takes the conformation TTT, GTG and TGT. The fibre periods of these models are similar. Therefore, it is not possible at present to select the best model to explain the observed fibre period of $\approx 20.5 \text{ \AA}$.

CALCULATION OF YOUNG'S MODULUS

Young's modulus was calculated based on the lattice dynamical theory^{2,3,11}, which requires both geometrical and force field information as input data to the computer system. For the geometrical data, the structural models constructed in the previous section were used. For the

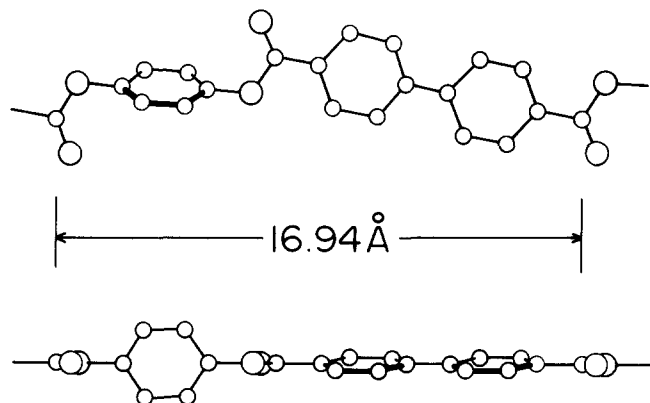


Figure 6 Molecular structure of model IV

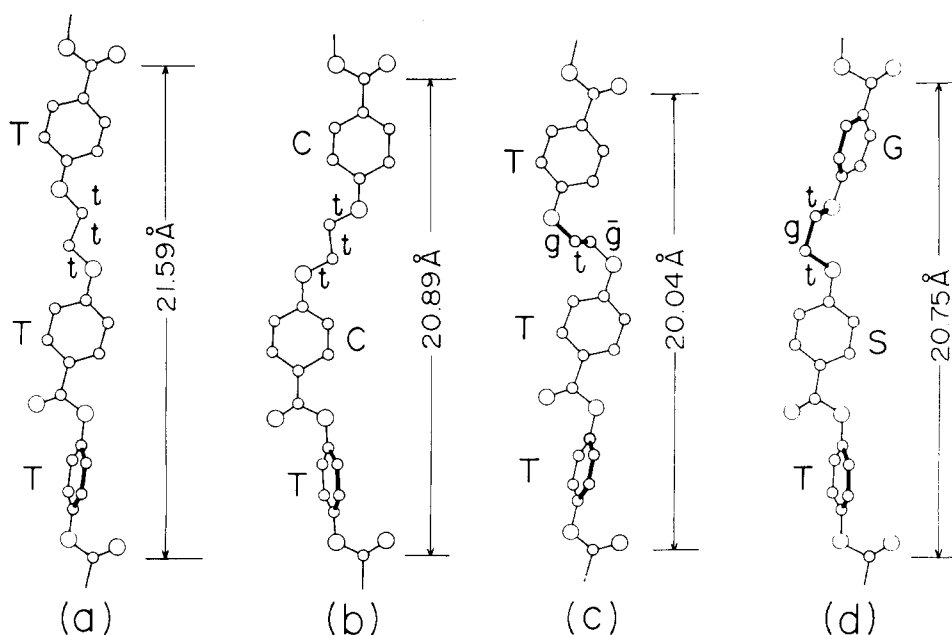


Figure 7 Molecular structure of model III

intramolecular force constants, the numerical values reported for various types of low molecular weight compound and polymer were transferred with some modifications (Table 2)².

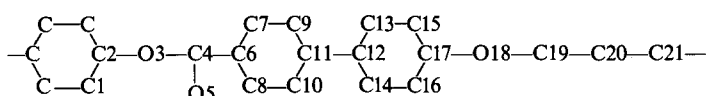
Figures 8 and 9 show, respectively, the infrared and far-infrared spectra taken for the POB whisker and Ekonol compared with the calculated wavenumbers of the normal vibrational modes. Agreement between observed and calculated wavenumbers is relatively good, indicating that the force constants used here are reasonable. Table 3 lists Φ and E_t values calculated thus, where Φ is extensibility and E_t is Young's modulus. Φ is defined as the force necessary to stretch the chain by 1% strain, i.e. $\Phi = E_t S \times 0.01$ (where S is the effective cross-sectional area of the chain), and is a measure of the rigidity of the polymer chain. Note that, in the calculation of the modulus E_t , a suitable cross-sectional area S must be assumed for each polymer. For the present arylate polymer samples, however, the poor X-ray reflection data make it difficult to estimate the unit cell constants or the effective cross-sectional area, except for POB^{4,5}. The S values of the aromatic polyesters, revealed by the X-ray structural analyses, are shown in Table 4. The data suggest that $S \approx 21 \text{ \AA}^2$ on average for the all *trans* structure (PEOB β form, PTMT β form and POB), and $23\text{--}25 \text{ \AA}^2$ for the structure containing *gauche* bonds (PEOB α form and PTMT α form). The S value of PET is a little larger than for the other *trans* types, possibly because of deviation from the planar zig-zag structure¹⁰.

From the data in Table 4, we can say that in general the cross-sectional area of the polyester chain is similar for many aromatic polyesters as long as their structures are not very different. This may also be reasonable from the viewpoint of van der Waals radii of the constituent atoms. Therefore, in the present calculations, a cross-sectional area of $21 \leq S \leq 24 \text{ \AA}^2$ is tentatively used as an approximation (Table 3). (In the application of these theoretical moduli to polymer samples 1–5, the effect of side groups such as phenyl, methyl or chlorine atoms must be taken into account because they may enlarge the cross-sectional area of the chain.)

Table 2 Force constants used for the calculation of Young's moduli of arylate polymers^a

Stretching (mdyn ^b Å ⁻¹)							
(1,2)	6.433	(2,3)	5.09	(3,4)	6.18	(4,5)	12.4
(4,6)	4.5	(11,12)	6.433	(18,19)	5.09	(19,20)	4.26
Bending (mdyn Å rad ⁻²)							
(2,3,4)	1.62	(3,4,5)	1.0	(3,4,6)	0.8		
(5,4,6)	0.6	(7,6,8)	0.934	(17,18,19)	1.3		
(18,19,20)	1.18						
Skeletal torsion and out-of-plane mode (mdyn Å rad ⁻²)							
(1,2,3,4)	0.03	(2,3,4,6)	0.23	(3,4,6,7)	0.23		
(6,7,9,11)	0.3	(17,18,19,20)	0.03	(18,19,20,21)	0.03		
(4,5) o.p.	0.58						
Stretch-stretch (mdyn Å)							
(1,2)-(2,3)	0.75	(2,3)-(3,4)	0.1	(3,4)-(4,6)	0.288		
(4,5)-(3,4)	0.3	(4,5)-(4,6)	0.3	(4,6)-(7,9)	-0.316		
(4,6)-(9,11)	0.342	(4,6)-(6,7)	0.75	(6,7)-(7,9)	0.75		
(6,7)-(9,11)	-0.316	(6,7)-(10,11)	0.342	(8,10)-(12,13)	0.342		
(10,11)-(11,12)	0.75	(10,11)-(12,13)	-0.316				
(17,18)-(14,16)	-0.316	(17,18)-(12,13)	0.342				
(18,19)-(19,20)	0.1						
Stretch-bend (mdyn rad ⁻¹)							
(2,3)-(2,3,4)	0.48	(3,4)-(3,4,6)	-0.3				
(3,4)-(2,3,4)	-0.3	(4,5)-(3,4,5)	0.65				
(4,5)-(6,4,5)	0.65	(4,6)-(4,6,7)	0.164				
(6,7)-(6,7,9)	0.164	(11,12)-(9,11,12)	0.164				
(17,18)-(16,17,18)	0.164	(18,19)-(17,18,19)	0.48				
(18,19)-(18,19,20)	0.62	(19,20)-(18,19,20)	0.4				
Bend-bend (mdyn Å rad ⁻²)							
(5,4,6)-(4,6,7)	0.11						

^a(*i, j*) and (*i, j, k*) denote bond *i-j* and $\angle ijk$, respectively, where *i, j* and *k* are atom numbers as illustrated below:



^b 1 dyn = 10⁻⁵ N

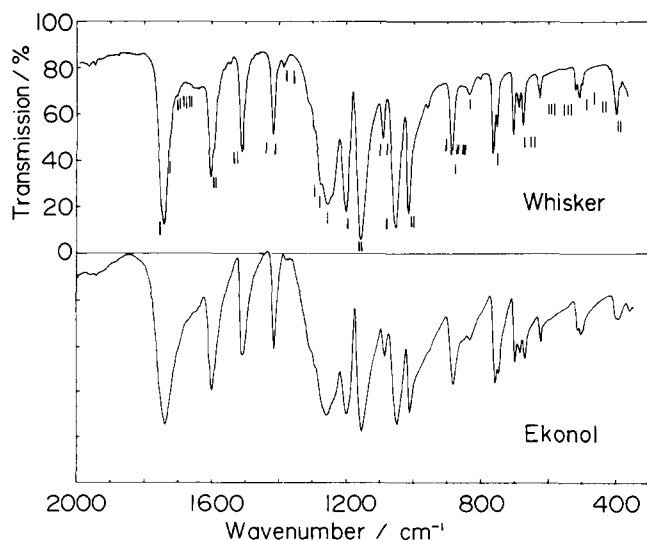


Figure 8 Infrared spectra of poly-*p*-oxybenzoyl whisker and the bulk sample (EkonoI). Vertical bars denote frequency positions calculated by normal-modes treatment

As seen in Table 3, for all models I-IV, the almost fully extended conformation gives a calculated Φ value of 3.4-3.7 $\times 10^{-10}$ N and a Young's modulus E_t of 150-180 GPa. In model I, the *trans*-planar structure gives a high value of E_t , 204 GPa. (The Young's modulus of the all *trans* structure model I was calculated by Ward *et al.*¹² to be 155 GPa based on the method of Treloar¹⁶. This value seems low, possibly because they used only the diagonal force constants in the calculation and did not take into consideration the interactions between the internal coordinates.) The small torsion from the *trans* structure results in a decrease of the modulus to 157 GPa. This value is considered to be the most plausible limiting modulus for POB crystal. The *cis*-planar structure gives a lower value of 137 GPa (105 GPa as calculated by Ward *et al.*¹²). The difference in E_t between *trans* and *cis* types is seen also for model III ($E_t = 154$ GPa for *trans* form and 59 GPa for *cis* form) and for poly-*p*-benzamide ($E_t = 238$ GPa for *trans* form and 163 GPa for *cis* form²). As stated in the previous section, models II and III have a chain structure essentially the same as that of model I, giving similar E_t and Φ values. Strictly,

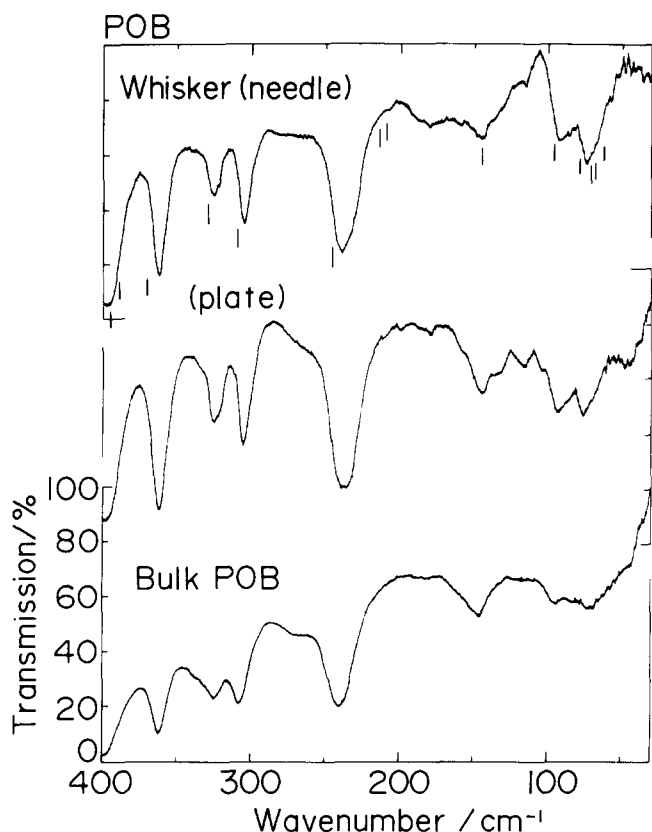


Figure 9 Far-infrared spectra of poly-*p*-oxybenzoyl whisker and the bulk samples. The whisker takes two types of crystal shape, needle and plate, whose spectra are shown separately here. Vertical bars denote the frequency positions calculated by normal-modes treatment

Table 3 Calculated Young's moduli for arylate polymers^a

Model	Φ (10^{-10} N)	E_1 (GPa)	S (\AA^2)
I torsion	3.28	157	20.9
I <i>trans</i>	4.26	204	
I <i>cis</i>	2.86	137	
II	3.74	178	21
III all <i>trans</i>	3.70	154	24
III <i>cis</i>	1.42	59	
III <i>gauche</i> -CH ₂	0.83	35	
IV	3.40	154	22

^a Φ , extensibility; E_1 , Young's modulus; S , effective cross-sectional area of chain

however, model IV, i.e. the polymer chain with the biphenyl group, gives a modulus a little higher than that of the corresponding polymer chain with a single benzene ring, model II. More detailed discussion follows in a later section.

For model III, introduction of methylene *gauche* bonds into the all-*trans* structure appreciably contracts the chain from the extended form, resulting in a decrease of the Young's modulus by an order of magnitude. A similar effect of the methylene *gauche* conformation can be clearly seen also for the PTMT α (10 GPa) and β (27 GPa) forms and PEOB α (2 GPa) and β (57 GPa) forms^{2,13,14}. As frequently observed, the *trans* conformation of the flexible methylene sequences tends to transform into the *gauche* conformation on heating to high temperature. Such a *trans*-*gauche* structural transformation

Table 4 Effective cross sectional area of aromatic polyesters

	S (\AA^2)	Molecular conformation
PET	24.7 ²	all <i>trans</i>
PTMT ^a (α)	22.5	<i>gauche</i>
(β)	20.7	all <i>trans</i>
PEOB (α)	24.9	<i>gauche</i>
(β)	20.6	all <i>trans</i>
POB	20.9	all <i>trans</i>

^aPTMT = poly(tetramethylene terephthalate)

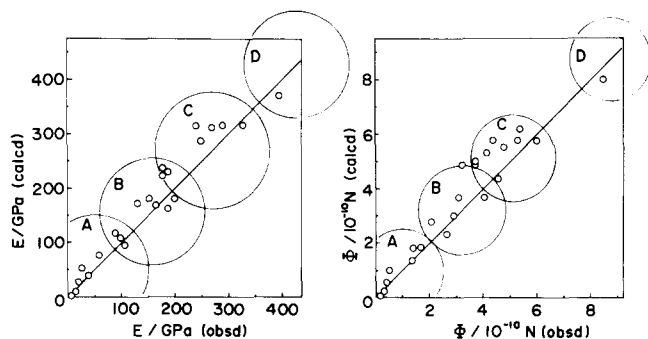


Figure 10 Relationship between calculated and observed crystallite moduli and extensibility for various kinds of polymer: A, helix glide; B, aramide, arylate; C, planar zig-zag; D, rigid rod linear polymer

is also expected to occur in the soft part of model III in the temperature region above the solid-liquid crystal transition point. The calculated result in Table 3 leads us to expect that the Young's modulus might decrease remarkably in such a transition temperature region.

Figure 10 shows a summary for the relationship between the calculated and observed E_1 and Φ values for many kinds of crystalline polymer. The observed values are based on measurements by the X-ray diffraction method^{*13,15}. The straight line with 45° slope indicates complete agreement between calculated and observed moduli. Figure 10 demonstrates that the lattice dynamical calculation gives, on the whole, a reliable Young's modulus. So, the lattice dynamical calculation provides us with a possible method to predict theoretically the mechanical properties of a newly conceived polymer chain. In other words, the lattice dynamical calculation may play an important role as a guiding principle for developing new polymer materials with excellent mechanical properties¹¹.

The polymers shown in Figure 10 are roughly classified into four groups:

- (1) helical and glide-type polymers;
- (2) aramide and arylate polymers;
- (3) planar zig-zag type;
- (4) heterocyclic linear polymers.

Referring to the calculated E_1 and Φ values in Table 3, the arylate polymers of models I-IV are included in group 2. The members included in group 2 have a chemical structure consisting of a repetition of the benzene and

* Jiang *et al.*¹⁵ proposed a limiting modulus of 450 GPa for PBT by extrapolating the X-ray observed moduli to the 'perfect crystal state'. But their calculation contains some assumptions concerning the modulus of the amorphous phase etc. and their idea of 'perfect crystal state' is unclear. In the present paper, therefore, 395 GPa is quoted from their experimental data, which is their maximal value actually measured by the X-ray diffraction method under the assumption of uniform stress distribution, as conventionally used.

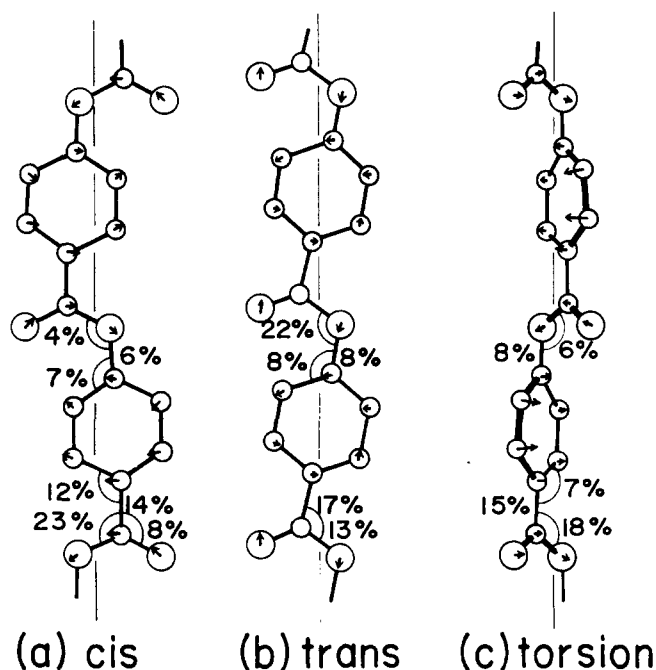


Figure 11 Calculated atomic displacements (inner strains)^{2,3} and potential energy distribution for model I: (a) *cis*; (b) *trans*; (c) torsion

ester (amide) groups. When the benzene ring is replaced by a virtual bond, the skeletal chain may be assumed to be a zig-zag conformation, having arms of different bond lengths². The present four polymers can be also considered to take a similar zig-zag type skeletal form and so possess moduli very similar to the other members of the group².

Molecular deformation mechanism

Figures 11–13 show atomic displacements (internal strain) and the distribution of strain energy (potential energy distribution, PED) among internal displacement coordinates such as bond lengths and bond angles, which are calculated for the arylate polymer chains subjected to a hypothetically large tensile deformation of 10%. For the *trans* and torsioned forms of the models I (Figure 11), II and IV (Figure 12), and the all *trans* type of model III (Figure 13), the atoms are displaced so that the virtual bonds passing through the benzene rings tend to rise vertically along the chain axis or into the drawing direction and correspondingly the strain energy distributes mainly to the deformation of angles $\angle O-C(O)-\phi$ and $\angle C(O)-O-\phi$ of the ester groups. Simultaneously, the stretching of the benzene-ester linkage and the intra-ring deformation of the benzene or biphenyl groups are also detected, although the PEDs are not as high. The torsional motion of the benzene ring also occurs around the virtual bond so as to elongate the twisted and contracted structure into the fully extended planar conformation. (A typical example can be seen in Figure 11c.)

Figure 14 shows the PEDs calculated for all *trans* polyethylene, poly-*p*-phenylene terephthalamide (Kevlar), and PBT (poly-*p*-phenylene benzobisthiazole^{2,11}). Just as in the arylate polymer cases, the Kevlar chain may be represented by the zig-zag conformation with different bond lengths when the bond passing through the benzene ring is assumed to be a virtual bond. The virtual bond is inclined from the vertical axis and then

the molecular deformation of such a zig-zag chain is induced by the bond-angle deformation of the zig-zag skeleton. That is, the strain energy does not distribute as much to the deformation of the benzene ring and, therefore, the rigidity of the benzene ring is not as effectively used as expected from the chemical structure. (The calculated modulus is 182 GPa.) A quite contrary case is seen for PBT in Figure 14c, where the rigid rings are connected almost in parallel along the chain axis and the strain energy is consumed directly by the deformation of the rings. PBT has a theoretical Young's modulus of 392 GPa, which is in good agreement with the X-ray observed value of 395 GPa¹⁵. (The theoretical Young's modulus of PBT was calculated to be 371 GPa in the previous paper¹¹. But we have now recalculated it in line with the above, by changing the value of the stretching force constant in the previous paper (the benzene-

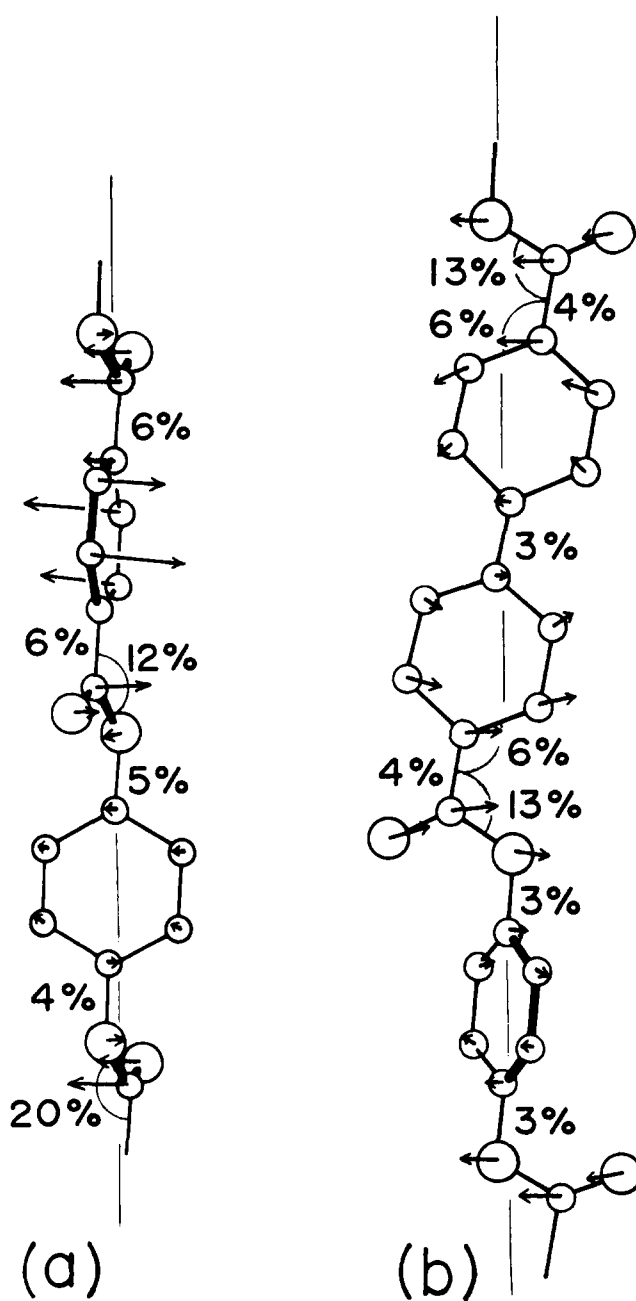


Figure 12 Calculated atomic displacements (inner strains) and potential energy distribution for models II (a) and IV (b)

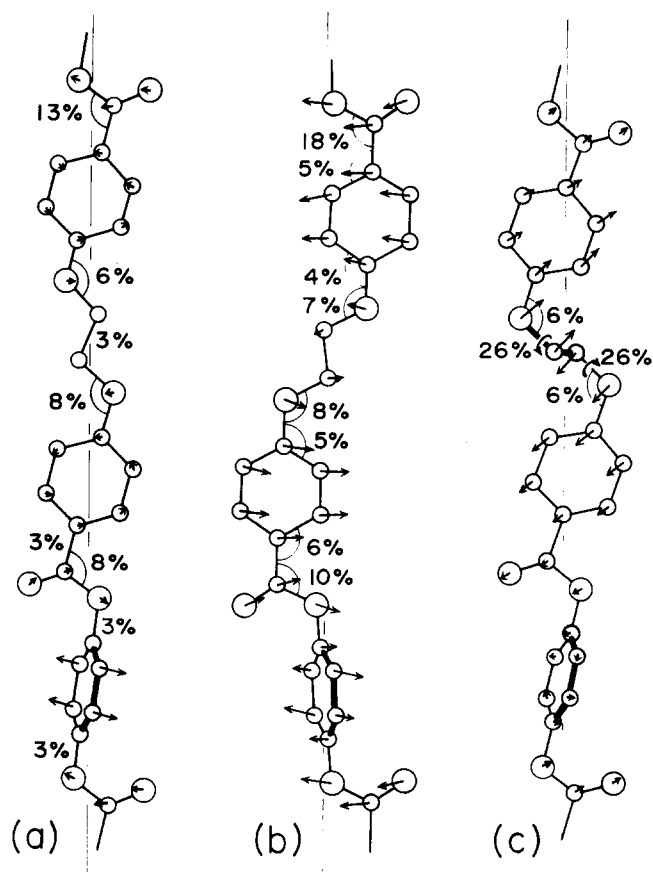


Figure 13 Calculated atomic displacements (inner strains) and potential energy distribution for model III with various types of methylene conformation

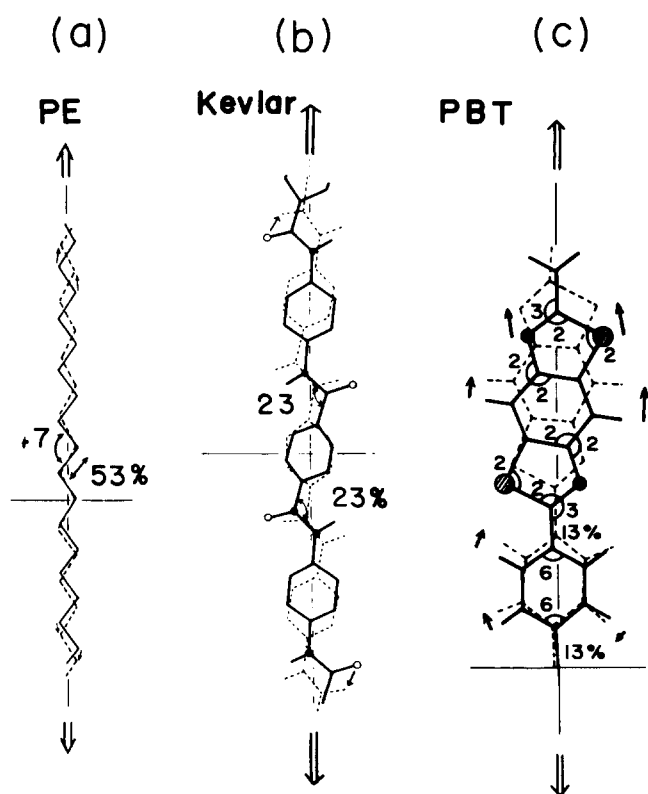


Figure 14 Calculated atomic displacements and potential energy distribution for (a) polyethylene, (b) poly-*p*-phenylene terephthalamide and (c) poly-*p*-phenylene benzobisthiazole^{2,3,11}

benzobisthiazole linkage 4–7; refer to Table 1 in Reference 11) from 4.4 to 5.5 mdyn Å⁻¹, because the latter force constant was considered more reasonable when taking into account the conjugated structure of the PBT chain.) As seen here, the zig-zag conformation of the aromatic polyamides and polyesters has some limiting effect on the modulus, in spite of the existence of rigid ring groups in the skeletal structure.

For *cis* type conformations such as those of models I (Figure 11a) and III (Figure 13b), the virtual bond of the benzene ring tends to be curved toward the centre line of the chain axis under the application of tensile force; such a bending of the skeleton has been reported also for *cis* type poly-*p*-benzamide². In the model of Figure 13c, i.e. model III with the methylene *gauche* bond, most of the potential energy distributes to the internal rotation of this flexible part and the torsional angles tend to change from *gauche* to *trans* position when the chain is stretched. Such PED and deformation mechanism result in the low Young's modulus of this polymer conformation model.

Effect of the length of phenylene rings on Young's modulus

Of the two extended polyesters of models II and IV, the modulus is a little higher for model IV. That is, a polymer with a diphenyl group in the skeletal chain may give a higher Young's modulus. So the question arises whether the modulus is higher for a polymer chain with a longer skeletal bond. We have calculated the effect of the sequential length of benzene rings upon Young's modulus E_1 . Figure 15 shows the model used in this calculation, where a series of benzene rings is replaced by a bond with length R_2 . The bond length of the ester C–O bond is R_1 and the bond angle is ϕ . The corresponding force constants are defined as K_2 , K_1 and H , respectively. Simple arithmetic gives the equations for the internal displacement coordinates (ΔR_1 , ΔR_2 and $\Delta\phi$), Young's modulus E_1 and the PED for this model^{16,17}:

$$\Delta R_1 = f(R_1 - R_2 \cos \phi) / (K_1 I)$$

$$\Delta R_2 = f(R_2 - R_1 \cos \phi) / (K_2 I)$$

$$\Delta\phi = fR_1 R_2 \sin \phi / (2HI)$$

$$1/E_1 = (S/I)[K_1(\Delta R_1/f)^2 + K_2(\Delta R_2/f)^2 + 2H(\Delta\phi/f)^2]$$

For ΔR_1

$$\text{PED} = K_1 \Delta R_1^2 / \Sigma$$

for ΔR_2

$$\text{PED} = K_2 \Delta R_2^2 / \Sigma$$

for $\Delta\phi$

$$\text{PED} = 2H \Delta\phi^2 / \Sigma$$

where $\Sigma = K_1 \Delta R_1^2 + K_2 \Delta R_2^2 + 2H \Delta\phi^2$, the fibre period $I = (R_1^2 + R_2^2 - 2R_1 R_2 \cos \phi)^{1/2}$ and f is the externally applied tensile force. Using suitable values for the parameters¹¹ ($R_1 = 1.37$ Å, $R_2 = 4.14n$ Å ($n = 1, 2, \dots$), $\phi = 110.9^\circ$, $K_1 = 6.0$ mdyn Å⁻¹, $K_2 = 1.55$ mdyn Å⁻¹ and $H = 0.8$ mdyn Å rad⁻²), the extensibility Φ and the potential energy distribution are calculated as shown in Figure 16. Figure 16a also shows the calculated result for the linear rod consisting of a series of benzene rings

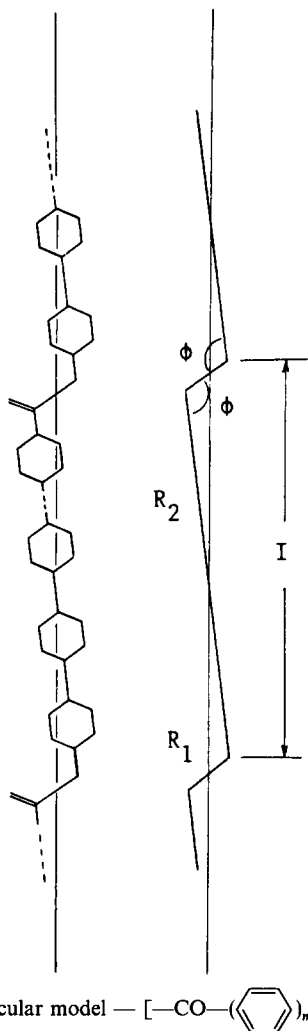


Figure 15 Molecular model $[-CO-(\text{C}_6\text{H}_4)_m-O-]$

(poly-*p*-phenylene), where the extensibility is given as

$$\Phi = R_2 K_2 \times 0.01$$

As seen here, the modulus increases linearly with bond length R_2 . But it is far lower than the modulus calculated for the completely linear case. In the limiting case of infinitely long R_2 , the ratio of the modulus to that of the straight chain is given by

$$\begin{aligned} & \left(\lim_{R_2 \rightarrow \infty} E_t \right) / [E_t(\text{linear})] \\ &= 1 / [1 + K_2 \cos^2 \phi / K_1 + K_2 R_1^2 \sin^2 \phi / (2H)] \\ &\approx 0.38 \end{aligned}$$

That is, the limiting modulus for the infinitely long R_2 model is only about one third that of the straight chain. This is because the zig-zag model used always contains some contribution from the bond-angle deformation, even for infinitely long R_2 . This deflection part at bond angle ϕ plays a significant role as a kind of defect in greatly reducing the modulus. This situation can be understood from Figure 10b. The PED for the bond angle deformation ($\Delta\phi$) is $\approx 60\%$ and the PED for the stretching (ΔR_2) is $\approx 40\%$. Therefore, we can say that the deformation of the chain is governed mainly by the bond-angle deformation mechanism. Only a small amount of a structural defect such as bond deflection is enough greatly to reduce the modulus. This result clearly indicates that the arylate polymers have an essential

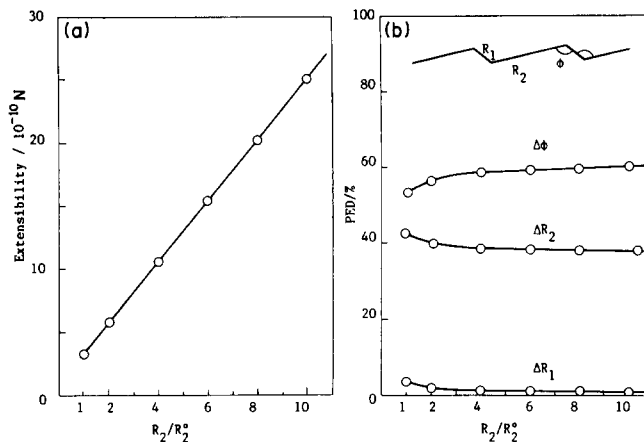


Figure 16 (a) Calculated extensibility and (b) potential energy distribution for the model shown in Figure 15 and the linear model of poly-*p*-phenylene; $R_2^0 = 4.14 \text{ \AA}$

limitation on increasing the modulus because of the existence of a deflection part, such as ester groups. So the arylate polymers discussed here may not be very useful for the industrial purpose of producing fibres with Young's modulus as high as possible. If we aim only to increase the modulus, we should use a completely linear polymer group such as PBT or poly-*p*-phenylene pyromellitimide, as discussed above (Figure 14)¹¹. But, as is well known, arylate polymers have the advantage of good processability by melting. As expected from Figure 16, an increase in the number of benzene rings in the skeletal chain may increase the modulus of the system but the long sequences of phenylene rings might decrease the melt processability.

CONCLUSIONS

We have presented Young's moduli calculated based on the lattice dynamical equations for a series of arylate polymers and interpreted the results from the molecular theoretical point of view in terms of atomic displacements and potential energy distribution. The all *trans* conformation gives a modulus of $\approx 155\text{--}180 \text{ GPa}$, irrespective of chemical structure. Introduction of *gauche* bonds into the flexible methylene segments reduces the modulus by an order of magnitude. The existence of ester groups causes a deflection of the straight skeletal chain, as seen in Figure 15, and limits the Young's modulus by about one third of that in the case of a fully straight linear chain. But the theoretically predicted modulus of arylate polyesters is comparable to that of amide polymers and so they could provide superior polymers with optimal properties of both good processability and high modulus.

ACKNOWLEDGEMENTS

We thank Toyobo Co. Ltd and Sumitomo Chemical Industry Co. Ltd Japan for supplying the samples of POB. We also thank the Research Association of Polymer Basic Technology in Japan for supplying the sample of liquid crystalline polymers (samples 2-5). This work was supported in part by a grant-in-aid from the Agency of Industrial Science and Technology, Ministry of International Trade and Industry of Japan.

REFERENCES

- 1 Chung, T-S. *Polym. Eng. Sci.* 1986, **26**, 901
- 2 Tashiro, K., Kobayashi, M. and Tadokoro, H. *Macromolecules* 1977, **10**, 413
- 3 Tashiro, K., Kobayashi, M. and Tadokoro, H. *Macromolecules* 1978, **11**, 908
- 4 Kato, Y., Endo, S., Kimura, K., Yamashita, Y., Tsugita, H. and Monobe, K. *Kobunshi Ronbunshu* 1987, **44**, 35, 41
- 5 Yamashita, Y., Nishimura, S., Fujiwara, Y., Monobe, K. and Shimamura, K. *Polym. Prepr. Jpn* 1983, **32**, 2589
- 6 Adams, J. M. and Morsi, S. E. *Acta Crystallogr.* 1976, **B32**, 1345
- 7 Casalone, G., Mariani, C., Mugnoli, A. and Simonetta, M. *Acta Crystallogr.* 1969, **B25**, 1741
- 8 Perez, S. and Brisse, F. *Acta Crystallogr.* 1976, **B32**, 470
- 9 Perez, S. and Brisse, F. *Acta Crystallogr.* 1976, **B32**, 1518
- 10 Tadokoro, H. 'Structure of Crystalline Polymers', John Wiley, New York, 1979
- 11 Tashiro, K. and Kobayashi, M. *Sen-i Gakkaishi* 1987, **43**, 78
- 12 Troughton, M. J., Unwin, A. P., Davies, G. R. and Ward, I. M. *Polymer* 1988, **29**, 1389
- 13 Tashiro, K. and Tadokoro, H. Crystalline polymers, in 'Encyclopedia of Polymer Science and Engineering, 2nd Edn', John Wiley and Sons, New York, 1989, and references therein
- 14 Tashiro, K., Nakai, Y., Kobayashi, M. and Tadokoro, H. *Macromolecules* 1980, **13**, 137
- 15 'The Materials Science and Engineering of Rigid-Rod Polymers', (Eds W. W. Adams, R. K. Eby and D. E. McLemore) MRS Symp. Proc. No. 134, Boston, 1988
- 16 Treloar, L. R. G. *Polymer* 1960, **1**, 95, 279, 290
- 17 Tashiro, K., Kobayashi, M. and Tadokoro, H. *Macromolecules* 1977, **10**, 731